

RatCAP: Miniaturized Head-Mounted PET for Conscious Rodent Brain Imaging

P. Vaska, C. L. Woody, D. J. Schlyer, S. Shokouhi, S. P. Stoll, J.-F. Pratte, P. O'Connor, S. S. Junnarkar, S. Rescia, B. Yu, M. Purschke, A. Kandasamy, A. Villanueva, A. Kriplani, V. Radeka, N. Volkow, R. Lecomte, and R. Fontaine

Abstract— Anesthesia is currently required for PET studies of the animal brain in order to eliminate motion artifacts. However, anesthesia profoundly affects the neurological state of the animal, complicating the interpretation of PET results. Furthermore, it precludes the use of PET to study the brain during natural behavior. The RatCAP tomograph (Rat Conscious Animal PET) is designed to eliminate the need for anesthesia in rat brain studies. It is a miniaturized full-ring PET scanner which is attached directly to the head, covering nearly the entire brain. RatCAP utilizes arrays of 2 mm x 2 mm LSO crystals coupled to matching avalanche photodiode arrays, which are in turn read out by full custom integrated circuits. Principal challenges have been addressed considering the physical constraints on size, weight, and heat generation in addition to the usual requirements of small-animal PET such as high spatial resolution in the presence of parallax error. A partial prototype has been constructed and preliminary measurements and optimization completed. Realistic Monte Carlo simulations have also been carried out to optimize system performance, which is predicted to be competitive with existing microPET systems.

I. INTRODUCTION

The use of anesthesia may significantly confound the interpretation of animal brain studies using PET [1-3]. While anesthetics are required to achieve artifact-free images by eliminating the possibility of animal motion in an ethical way, they may profoundly disturb the neurological systems under study. Furthermore, anesthesia largely precludes the use of PET to study the neurological changes associated with normal behavior. The ability to perform PET scans of the conscious animal brain would be a great advance in neuroscience, by both improving the quality of current studies as well as by opening up a whole new research area of behavioral studies with PET.

In the case of the rat brain, a novel solution was recently proposed [4], dubbed RatCAP (Rat Conscious Animal PET). The approach is to miniaturize the PET scanner and attach it directly to the head of the rat, permitting movement of the animal while eliminating any relative motion between the scanner and head. A mockup is shown in Fig. 1. While

retaining standard scintillation crystal technology, the size reduction is made possible by using wafer-thin silicon avalanche photodiode (APD) arrays as photosensors and custom integrated circuits (IC) to perform front-end signal processing.



Figure 1. Full-size prototype of mechanical frame for the RatCAP scanner in place on the head of a rat (left), and its support structure with counterbalanced arm and electronically controlled rotating bowl enclosure for the rat (right).

The current design consists of a ring of 12 detector blocks, each comprising a 4 x 8 array of cerium-doped lutetium oxyorthosilicate (LSO) crystals with 2 mm x 2 mm cross-section and 5 mm length, coupled to a matching S8550 APD array (Hamamatsu Photonics, Japan). A schematic diagram displaying these components is shown in Fig. 2. The specialized application and scanner geometry pose significant challenges in terms of both animal compatibility and the usual requirements of quantitative brain PET such as high spatial resolution and sensitivity.

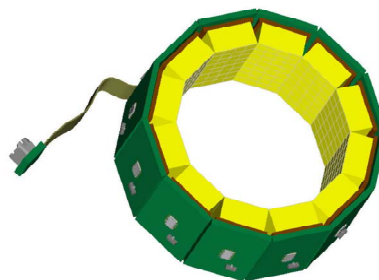


Figure 2. Schematic rendering of RatCAP without its mechanical frame, depicting LSO arrays (yellow), APD arrays (brown), and readout electronics on printed circuit boards (green).

Manuscript received October 29, 2003. This work was supported by the U.S. Department of Energy (OBER) under Prime Contract No. DE-AC02-98CH10886.

Most authors are with Brookhaven National Laboratory, Upton, NY 11973 USA (telephone: 631-344-6228, e-mail: vaska@bnl.gov).

N. Volkow is with the National Institutes of Health, Bethesda, MD USA, on leave from Brookhaven National Laboratory (e-mail: volkow@bnl.gov).

R. Lecomte and R. Fontaine are with Dept. of Electrical and Computer Engineering, Universite de Sherbrooke, Sherbrooke, Quebec J1K 2R1.

II. ANIMAL COMPATIBILITY

The LSO/APD detector blocks are approximately 1 cm transaxially and 2 cm axially. Fig. 1 shows that the scanner is small enough to allow normal vision and posture. Fig. 3 displays a rat brain scan obtained from a microPET scanner (Concorde Microsystems, Knoxville, TN) with the RatCAP geometry superimposed, showing that this position covers nearly the whole brain. An inner sleeve, with an inner diameter of 37 mm, will first be mounted permanently to the skull with procedures similar to those used for implanting rat brain probes, and the tomograph will be mounted to the sleeve only during conditioning of the animal and scanning.

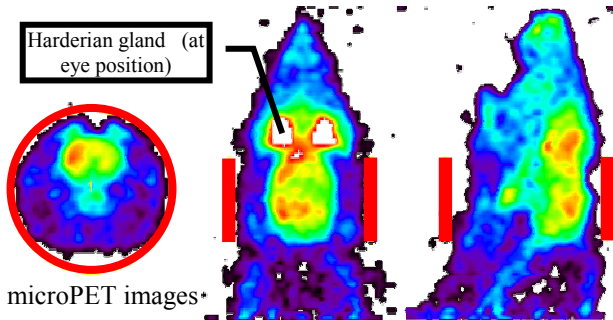


Figure 3. RatCAP mounting position superimposed on microPET images: transverse, coronal, and sagittal slices through a rat brain from a ^{11}C -raclopride study acquired on a Concorde microPET R4 scanner. The position of the proposed RatCAP inner sleeve is shown in red, to scale.

For freedom of movement, the ring is designed to pivot freely around multiple axes, and the weight of the tomograph will be supported from above by a tether attached to a counterweighted, pivoting arm as shown in Fig. 1. Nevertheless, the mass must be minimized to allow the rat to overcome the added inertia from the device (~ 150 g) which is a significant fraction of the weight of a typical laboratory rat (~ 300 g). The tolerance of the ring by lab rats, which involves gradual conditioning to the device, is being investigated.

III. DETECTOR DESIGN AND OPTIMIZATION

A platform for mounting 2 blocks has been constructed, allowing precise control over detector alignment, separation distance, and rotation of phantoms about the symmetry axis between them for preliminary imaging studies, as shown in Fig. 4. The data acquisition system independently processes all 64 channels of the 2 blocks, using hybrid preamps, shaping amplifiers, and CAMAC-based LeCroy FERA/ECL constant-fraction discriminators and ADCs. Coincidence logic was performed with NIM hardware, and KMaxNT software (Sparrow Corp., Starkville, MS) used for data acquisition.

Several different block designs were studied in terms of absolute light output (primary APD photoelectrons per MeV) and FWHM energy resolution at 511 keV. Designs by Proteus (Chagrin Falls, OH) used a radiant mirror foil

reflector (3M, St. Paul, MN) and were tested in 5 and 10 mm lengths, with and without gluing on the reflector. Blocks from CTI (Knoxville, TN) used a powder reflector. Table 1 shows that the Proteus blocks with only the entrance face glued give the best light output and energy resolution. Note that the final IC electronics are expected to give better performance since, in contrast to the current readout system, they are specifically designed for these detectors. More details are provided in [5]. Preliminary time resolution measurements with a ^{22}Na source yielded 2.8 ns FWHM between a selected detector in the block and a BaF₂ detector which is comparable to existing tomographs.

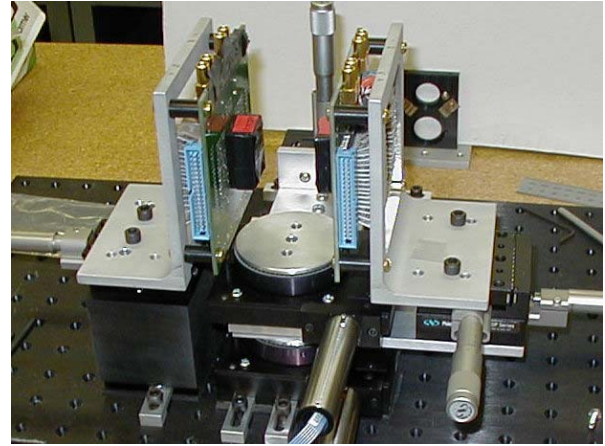


Figure 4. Prototype data acquisition setup for RatCAP, with 2 opposing detector blocks inside light-tight holders (black) and mounted on preamp boards, a computer-controlled turntable between the blocks, and various adjustments for accurate alignment. Connection cables have been removed for clarity.

TABLE 1. MEASURED PERFORMANCE OF VARIOUS DETECTOR BLOCK CONFIGURATIONS.

make	length (mm)	construction	photo-electrons/MeV	FWHM resolution (%)
CTI	8	slotted block	2918	25
Proteus	5	glued	1513	20
	10	glued	2356	19
Proteus	5	no glue	3113	19
	10	no glue	2455	17
Proteus	5	end glued	4491	16

IV. READOUT ELECTRONICS DESIGN

Due to extremely limited space and power, the front-end processing for each block will be performed by a single, custom-designed 32-channel 0.18 μm CMOS application-specific integrated circuit (ASIC) [6]. The maximum power budget is 125 mW and an estimated final size is $1.5 \times 4.2 \text{ mm}^2$. The ASIC will perform preamplification, shaping, and programmable-level zero-cross discrimination independently for each crystal in the block. To minimize interconnections, the data output from each chip is a single multiplexed serial line. Every event above a programmable threshold produces a sequence of logic pulses on the serial line starting with a leading edge which is in phase with the occurrence of the event (but asynchronous to the system clock), followed by a synchronous 5-bit address encoding the crystal of interaction. The 12 data lines will be fed into a custom-designed VME module which time stamps the leading edge to $<2 \text{ ns}$ accuracy and packages the time stamp with a unique crystal address in a 64-bit word for VME readout to an acquisition PC.

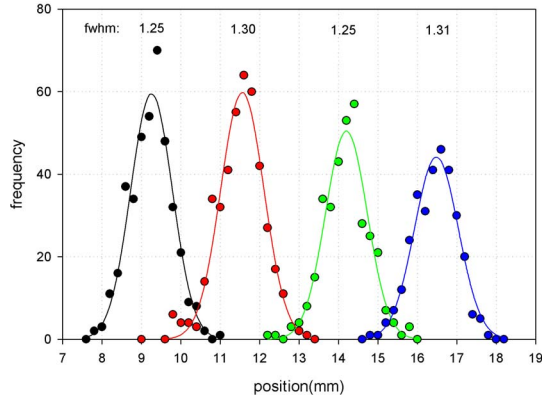


Figure 5. Intrinsic spatial resolution measurement for the Proteus block with 5 mm crystal length.

Note that no coincidence processing will be done during data collection. While this results in simplified data acquisition electronics, all singles events must be saved to disk for offline processing, resulting in potentially high data collection rates. Thus the readout system has been designed with a conservative maximum throughput goal of $\sim 1 \text{ Mcps}$ per block, which would result in a total data rate of 768 Mbps (within the realm of gigabit ethernet). However, more realistic estimates are at least a factor of ten below this. For example, a detector block with 10 mm long crystals measured a singles rate of only 50 kcps in contact with the head of a rat, 40 minutes after injection of 750 μCi of ^{18}F -FDG. This would generate data at a rate of 5 MB/s which, if sustained over a 60-min PET study, would produce a manageable 16 GB of singles data. Deadtime associated with multiplexing the 32 channels of the chip into a single line is calculated to be 6% at 1 Mcps, with a 100 MHz system clock, and substantially less than 1% at the lower, more realistic rates.

Randoms estimation can be easily performed offline using the standard delayed-coincidence method.

Another deviation from standard PET data acquisition is the lack of ADCs to perform energy measurement. ADCs were sacrificed because of IC power limitations imposed to prevent excessive heating. Temperature fluctuations could affect APD gain and possibly animal behavior. The individually-programmable discriminator thresholds will serve the same ultimate purpose of energy gating, although less conveniently because energy spectra can be created only by recording count rates as a function of threshold setting and differentiating the resulting spectrum. The more subtle consequences of omitting ADCs were studied [7] and the net effect estimated to be a $\sim 30\%$ loss in coincidence sensitivity, which was deemed a tolerable trade-off for the simpler, smaller, and cooler-running design. Analog outputs for each channel are being considered so that energy information may be determined by off-chip ADCs for future applications.

V. PRELIMINARY SYSTEM STUDIES

A. Spatial Resolution

The intrinsic spatial resolution of the detectors was measured by recording the coincidence rate as a $<1 \text{ mm}$ diameter ^{22}Na point source was moved across a row of detectors in steps of 0.2 mm. The result is shown in Fig. 5, and the average peak FWHM was 1.28 mm with no corrections for source size, positron range, or photon acollinearity. This compares favorably to the value of 1.75 mm measured for the Concorde microPET P4 [8] and 1.58 mm for the UCLA prototype microPET [9]. The modest improvement is most likely due to the direct coupling of the crystal to the photosensor (APD) in the RatCAP block.

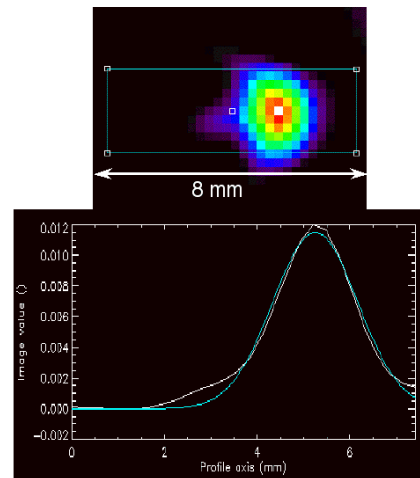


Figure 6. Measured image of 1 mm diameter ^{68}Ge point source (in steel casing) rotated between the 2-block prototype system at a radius of 1.6 mm (top), and Gaussian fit of profile (bottom). Filtered backprojection with ramp filter were used.

The system spatial resolution at the center is mostly determined by the cross-sectional size of the crystals. The chosen 2 mm size is essentially the same as in the Concorde microPET, and hence a similar resolution of 1.8 mm FWHM is expected at the center of the FOV. Using the prototype RatCAP system, a 1 mm diameter point source was placed 1.6 mm from the center and rotated about the center in a series of acquisitions to complete a fully tomographic data set. Fig. 6 shows the reconstructed image from which a resolution of 2.1 mm FWHM was measured. Details are provided in [10].

However, since the rat head nearly fills the entire FOV, parallax error is expected to be much more significant at off-center locations resulting in poorer radial resolution. Because the prototype has only 2 blocks and a limited adjustment for the angle between them, tomographic measurements could not be made at relatively large radii.

Hence simulations were used to predict the resolution across the entire FOV. The SimSET Monte Carlo package [11] was modified to accept a discrete-crystal annulus geometry closely approximating the RatCAP design [10]. Point sources were generated over a range of radii, and the data binned into direct-plane sinograms which were normalized and then reconstructed using filtered backprojection. The resolutions for 5 and 10 mm crystal lengths are shown in Fig. 7. The 5 mm length was selected for the final design to maintain resolution better than 2 mm throughout the brain at some expense of sensitivity.

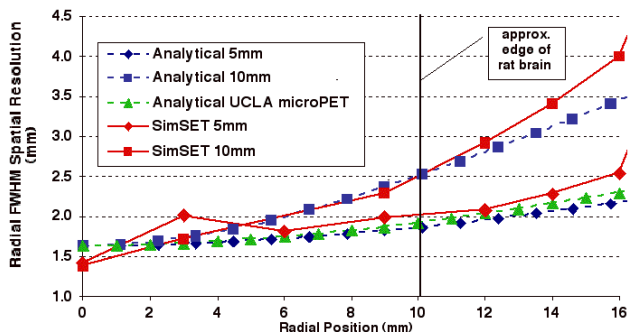


Figure 7. Simulated spatial resolution across FOV for RatCAP geometry with specified crystal lengths, and for the UCLA microPET as a comparison (more approximate, analytical results are from [4]).

B. Sensitivity

The coincidence sensitivity is a function of both the intrinsic detector sensitivity and the ring geometry. Despite an axial FOV of only 2 cm, the small ring diameter of the RatCAP provides a rather large acceptance angle of more than 25 degrees. As shown in Fig. 8, this is comparable to the Concorde microPET and considerably larger than that of the UCLA system. The loss in sensitivity from using shorter 5 mm crystals will be recovered in future designs by a second layer of crystals.

The coincidence sensitivity was measured with a 0.79 μCi ^{22}Na point source centered within the 2-block prototype. The true source activity was measured in a calibrated well counter, with a narrow energy window around the 511 keV photopeak in order to preserve its calibration in the presence of the 1275 keV gamma-ray. The coincidence rate between the 2 blocks with a threshold of ~ 400 keV was 18 cps. Coincidences due to randoms and LSO background radiation were negligible due to the weak source and high threshold, respectively. Extrapolating to a full ring system, the sensitivity would be 150 cps/ μCi or 0.41 %. This is consistent with the value of 1.86 % measured for the Concorde R4 system at this threshold [12] in that the R4 has similar solid angle, but crystals twice as long (10 mm) resulting in an expected ratio in coincidence of approximately 4.

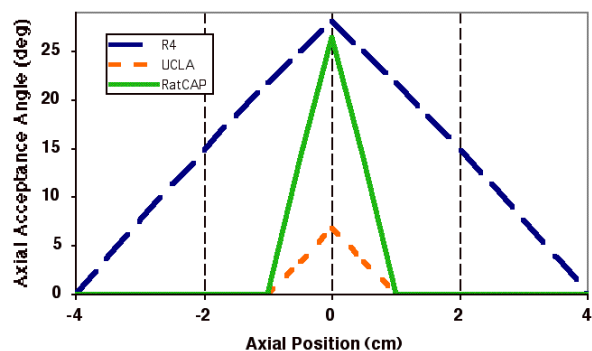


Figure 8. Axial acceptance angle as a function of position along scanner axis for Concorde microPET R4, UCLA microPET prototype, and RatCAP scanners.

C. Quantitative Corrections

Randoms will be minimized by using a narrow coincidence time window, enforced during offline software filtering of the saved, time-stamped singles events. The measured detector time resolution of 2.8 ns FWHM vs. a fast BaF_2 detector translates to an expected system resolution of ~ 4 ns FWHM, implying that a 10 ns time window is achievable. A narrow time window like this would cause some true coincidences to be rejected due to varying time delays among channels at the level of about a nanosecond. To minimize these losses, the time window will be shifted appropriately for each crystal pair. The shift can be determined by creating a time-difference spectrum for the detector pair and measuring the shift which centers the time window over the prompt coincidence peak. Randoms accepted within the time window will be estimated and subtracted using the widely accepted and accurate delayed-coincidence technique, which is easily applied to the singles data.

Scatter and attenuation corrections are simplified by the fact that their distributions will be very similar for each scan due to the close fit of the scanner to the head and the similarity of scattering medium among scans. Scatter acceptance will be minimized by a high discriminator threshold of ~ 400 keV which is acceptable based on the

measured energy resolution of 16 %. Deadtime is expected to be low as described above, but if necessary, standard correction schemes based on measured singles rates will be developed. Sinogram normalization strategies are under development.

D. Image Reconstruction

While the standard filtered backprojection algorithm has been used in the preliminary work, iterative image reconstruction algorithms are expected to be superior in that noise and resolution properties can be incorporated. Furthermore, gaps between blocks will be handled more effectively since continuous sampling is not assumed. The small total number of crystals (384) and small field of view imply that a totally uncompressed system matrix may be stored on disk (or possibly even in memory) and that reconstruction times will be reasonable. For example, the full system matrix would require less than 4 GB, assuming 1 mm cubic voxels throughout the entire FOV and 2-byte matrix elements. For the same reasons, the system matrix itself can be created with actual measurements or Monte Carlo simulations within a reasonable amount of time, offering potentially greater accuracy than analytical calculations and their accompanying approximations.

VI. CONCLUSIONS

The main components of the RatCAP tomograph design have been finalized. The mechanical frame and support structure are in advanced stages of development. The LSO crystal arrays will be of the Proteus design in 5 mm length, with 3M reflectors and no glue between crystals. The ASIC development has already been through multiple production cycles including testing and debugging, and a final design is underway. Energy and time resolution of the detector blocks are excellent. Preliminary measurements with a 2-block system as well as realistic Monte Carlo simulations of the whole tomograph indicate that tomographic performance will be competitive with existing systems, with the small size promising efficient use of sophisticated reconstruction algorithms.

VII. ACKNOWLEDGMENT

The authors are grateful to members of the BNL PET group for support with radioisotopes and animal issues.

VIII. REFERENCES

- [1] C. W. Berridge and M. F. Morris, "Amphetamine-induced activation of forebrain EEG is prevented by noradrenergic beta-receptor blockade in the halothane-anesthetized rat," *Psychopharmacology (Berl)*, vol. 148, pp. 307-313, 2000.
- [2] A. E. Ryabinin, Y. M. Wang, R. K. Bachtell, A. E. Kinney, M. C. Grubb, and G. P. Mark, "Cocaine- and alcohol-mediated expression of inducible transcription factors is blocked by pentobarbital anesthesia," *Brain. Res.*, vol. 877, pp. 251-261, 2000.
- [3] K. S. Hendrich, P. M. Kochanek, J. A. Melick, J. K. Schiding, K. D. Statler, D. S. Williams, D. W. Marion, and C. Ho, "Cerebral perfusion during anesthesia with fentanyl, isoflurane, or pentobarbital in normal rats studied by arterial spin-labeled MRI," *Magn Reson Med*, vol. 46, pp. 202-206, 2001.
- [4] P. Vaska, D. J. Schlyer, C. L. Woody, S. P. Stoll, V. Radeka, and N. Volkow, "Imaging the Unanesthetized Rat Brain with PET: A Feasibility Study," *2001 IEEE NSS/MIC Conference Record*, vol. M9A-8, 2001.
- [5] A. Kriplani, S. P. Stoll, D. J. Schlyer, S. Shokouhi, P. Vaska, A. Villanueva, and C. L. Woody, "Light Output Measurements of LSO Single Crystals and 4x8 Arrays: Comparison of Experiment with Monte Carlo Simulations," presented at 2003 IEEE Medical Imaging Conference, Oct. 19-26, Portland, OR, 2003.
- [6] J.-F. Pratte, G. De Geronimo, S. Junnarkar, P. O'Connor, B. Yu, S. Robert, V. Radeka, C. L. Woody, S. P. Stoll, P. Vaska, R. Lecomte, and R. Fontaine, "Front-end electronics for the RatCAP mobile animal PET scanner," presented at 2003 IEEE Medical Imaging Conference, Oct. 19-26, Portland, OR, 2003.
- [7] P. Vaska, S. P. Stoll, C. L. Woody, D. J. Schlyer, and S. Shokouhi, "Effects of Inter-Crystal Cross-Talk on Multi-Element LSO/APD PET Detectors," *IEEE Trans. Nucl. Sci.*, 2003 (in press).
- [8] Y. C. Tai, A. Chatzioannou, S. Siegel, J. Young, D. Newport, R. N. Goble, R. E. Nutt, and S. R. Cherry, "Performance evaluation of the microPET P4: a PET system dedicated to animal imaging," *Phys. Med. Biol.*, vol. 46, pp. 1845-1862, 2001.
- [9] A. F. Chatzioannou, S. R. Cherry, Y. Shao, R. W. Silverman, K. Meadors, T. H. Farquhar, M. Pedarsani, and M. E. Phelps, "Performance Evaluation of microPET: A High Resolution Lutetium Oxyorthosilicate PET Scanner for Animal Imaging," *J. Nucl. Med.*, vol. 40, pp. 1164-1175, 1999.
- [10] S. Shokouhi, P. Vaska, D. J. Schlyer, S. P. Stoll, A. Villanueva, A. Kriplani, C. L. Woody, and N. Volkow, "System Performance Simulations of the RatCAP Awake Rat Brain Scanner," presented at 2003 IEEE Medical Imaging Conference, Oct. 19-26, Portland, OR, 2003.
- [11] T. K. Lewellen, R. L. Harrison, and S. Vannoy, "The SimSET program," in *Monte Carlo Calculations in Nuclear Medicine, Medical Science Series*, M. Liungberg, S.-E. Strand, and M. A. King, Eds. Bristol: Institute of Physics Publishing, 1998, pp. 77-92.
- [12] C. Knoess, S. Siegel, A. Smith, D. Newport, N. Richerzhagen, A. Winkeler, A. Jacobs, R. N. Goble, R. Graf, K. Wienhard, and W. D. Heiss, "Performance evaluation of the microPET R4 PET scanner for rodents," *Eur J Nucl Med Mol Imaging*, vol. 21, pp. 21, 2003.